Scientific paper

Smeared-crack Modeling of R/ECC Membranes Incorporating an Explicit Shear Transfer Model

Benny Suryanto[1], Kohei Nagai[2] and Koichi Maekawa[3]

Received 16 March 2010, accepted 23 September 2010

Abstract

This paper presents the verification of analytical modeling for reinforced Engineered Cementitious Composite (R/ECC) in the context of a smeared, fixed crack approach. Verification is provided through the analysis of six R/ECC panels subjected to pure shear. The results demonstrate that the proposed models are capable of replicating various responses of the panels well, provided that tensile property of the ECC is calibrated against those obtained from the panel tests. These responses include load-deformation responses, the magnitudes and directions of principal stress and principal strain, and failure modes. The results also demonstrate the possibility of representing the average crack-shear transfer in the ECC with an explicit smeared model. Finally, this paper includes predictions of the shear capacity of R/ECC panels with a wide range of reinforcement ratios and concludes with discussions regarding factors influencing shear strength.

1. Introduction

The simulation of reinforced ECC (R/ECC) structural members can present a considerable challenge due to nonlinear material behavior. Yielding of the reinforcement and cracking of the ECC are often the prime source of nonlinearity in R/ECC. While the nonlinearity induced by reinforcement yielding is predictable and considerably dominates the structural response at high stresses, the nonlinearity induced by cracking in the ECC is dominated by low and high stresses. Consider, for example, the behavior of cracked ECC at the web region of a shear-critical beam shown in **Fig. 1**. When loaded, diagonal shear cracks may form at the web region of the beam, crossing the longitudinal and web reinforcements. Since the amount of longitudinal and web reinforcement is typically different, not only tensile stresses, but also shear stresses can present across cracks in the ECC. Depending on how these stresses are transmitted across the cracks, different stress carrying mechanisms can develop in the beam and affect its response significantly.

To predict the response of the beam illustrated, it is crucial to obtain a complete understanding of the mechanism of stress transfer in the cracked ECC. This includes compressive stress transfer parallel to cracks as well as tensile and shear stresses transfer across cracks. Nevertheless, behavioral aspects pertaining to crack-shear transfer has received comparatively little attention. To fill this knowledge gap, the authors conducted experiments on pre-cracked ECC plates subjected to principal stress rotation (Suryanto *et al* 2010a). It was demonstrated that, when the direction of principal tensile stress is changed, new cracks formed nearly orthogonal to the pre-existing cracks. The orthogonal crack pattern indicates that significant anisotropy is exhibited due to a lack of crack-stress transfer. While the stress-strain obtained from the experiments is useful for the modeling of ECC, direct observations on the mechanism of stress transfer of ECC in R/ECC members with ordinary reinforcement ratios are desirable. This is required as the reinforcement in R/ECC can dictate the overall member response and influence the response of the ECC.

In this paper, the mechanism of stress transfer in R/ECC is investigated from recent experiments on orthogonally-reinforced ECC panels tested at the University of Toronto (Xoxa 2003). The R/ECC panels tested can be regarded as a part of large R/ECC structures having uniform thickness and property, subjected to an in-plane stress field as illustrated in **Fig. 1(b)**. They were of similar dimension to those of reinforced concrete (RC) panels tested previously by Vecchio and Collins (1982) and Vecchio *et al* (1994), for instance. Since the stress states in the RC panel tests were uniform and well defined, the test results have provided an improved understanding of nonlinear mechanics of RC. This allows researchers to develop a general theory for RC and to verify analytical models they developed (Vecchio and Collins 1986, Cervenka 1985, Kaufmann and Marti 1998, Maekawa *et al* 2003, among others). Herein it will be shown that the results of the R/ECC panel tests are useful to investigate the nonlinear mechanics of R/ECC and to verify analytical modeling. Panel tests are referred to as such a test enables the consideration of inherent interaction between ECC and embedded reinforcement and the measurement of average stresses and average strains of the ECC.

[1]JSPS Postdoctoral Research Fellow, Department of Civil Engineering, University of Tokyo, Japan.
E-mail:benny@concrete.t.u-tokyo.ac.jp
[2]Lecturer, Department of Civil Engineering, University of Tokyo, Japan.
[3]Professor, Department of Civil Engineering, University of Tokyo, Japan.

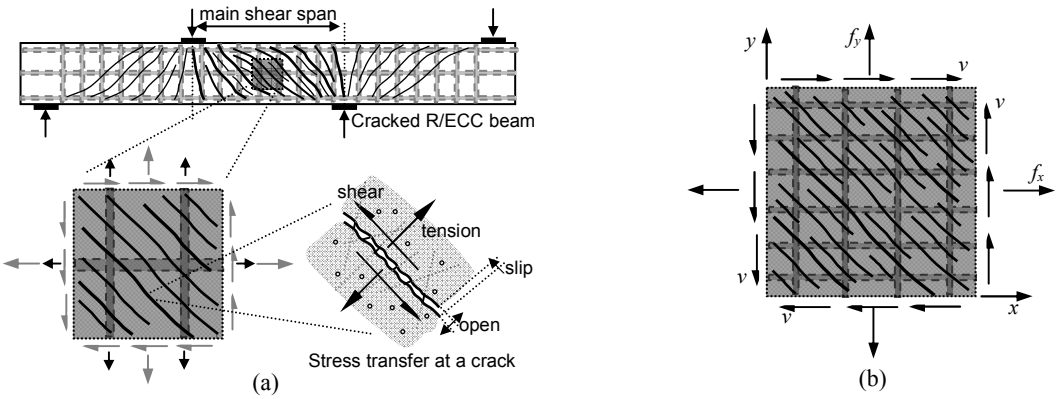

Fig. 1 Illustration of stress transfer across cracks in R/ECC: (a) R/ECC shear beam subjected to loading and (b) R/ECC membrane subjected to in-plane stresses.

Recently, the authors proposed a nonlinear finite element procedure in the context of a smeared, fixed crack approach for predicting the response of shear-critical members in a companion paper (Suryanto *et al* 2010b). The procedure has been shown to be applicable for predicting the response of damaged ECC plates subjected to principal stress rotation and shear-critical R/ECC beams under reversed cyclic loading. In both cases, significant deviation of principal stress and principal strain directions was observed even before the formation of crack localization. The procedure proposed differs to the smeared-rotating crack approach, which assumes the coincidence of stress and strain directions, adopted by Han *et al* (2003) and Suwada and Fukuyama (2006), for instance. It also differs to the one adopted by Hung and El-Tawil (2009) in which a hybrid rotating/fixed-crack approach is used (the fixed crack assumption is considered after a crack localization form). In this paper, the procedure proposed is used to evaluate the response of six R/ECC panels, focusing on the comparison between the computed and observed stress and strain fields of the ECC. To provide a comprehensive discussion, this paper includes: 1) a brief explanation of modeling of R/ECC in a smeared context, 2) verification study of the models based on the results of R/ECC panel tests, and 3) shear strength prediction of R/ECC based on the proposed models incorporating the identified tensile properties from the panel tests.

2. Modeling of R/ECC in a smeared approach

Nonlinear behavior of R/ECC is constructed by combining the behavior of reinforcement and cracked ECC in a smeared manner. The smeared concept allows a simple yet accurate representation of ECC behaviors without considering local ECC behavior at every single crack in the ECC. Cracked ECC is treated as an anisotropic material where the in-plane behavior can be represented by three smeared models that include compression, tension, and shear transfer models. The two-dimensional smeared models of RC described in Maekawa *et al* (2003) are used as the base models. To adapt the models for R/ECC, the formulations that describe the monotonic response are modified, whereas those describing the internal unloading-reloading loops are directly adopted as they are found to be applicable for ECC with PVA fibers 2% by volume that commonly used in practice. The internal loop may, however, not be applicable for different fiber types and volume fractions and hence further verification is necessary. In this section, the summary of the modified models is given, with more details described in a companion paper (Suryanto *et al* 2010b). The models are intended for the simulation of R/ECC members subjected to a limited number of load cycles.

For modeling of the behavior of reinforcement embedded in ECC, a simple elastic-plastic model is adopted as shown in **Fig. 2(d)**. This model is considered based on test observations reported by Fischer and Li (2002) that clearly demonstrated that the reinforcement deformation embedded in ECC is compatible with the surrounding ECC. As such, local stress-strain response of the reinforcement is thought to closely resemble its average stress-strain response. The hysteretic response of the reinforcement is modeled after Kato (1978), which is based on the cyclic response of bare reinforcement.

The modeling of cracked ECC in compression is based on the elasto-plastic model for cracked concrete. For ECC, the strain corresponding to the compressive strength ε_c' is shifted from a typical value of about 0.2% for concrete to approximately 0.5% [see **Fig. 2(e)**]. The weakening effects of transverse cracking are accounted by a reduction factor ω_c [**Fig. 2(h)**] and suggested to cause both stiffness and strength reductions to the compressive response.

The modeling of cracked ECC in tension is assumed to follow a tri-linear model [see **Fig. 2(f)**]. The weakening effects of transverse cracking are accounted by a reduction factor ω_t shown in **Fig. 2(i)**. The factor is used to reflect the disturbance of the transverse cracks to fi-

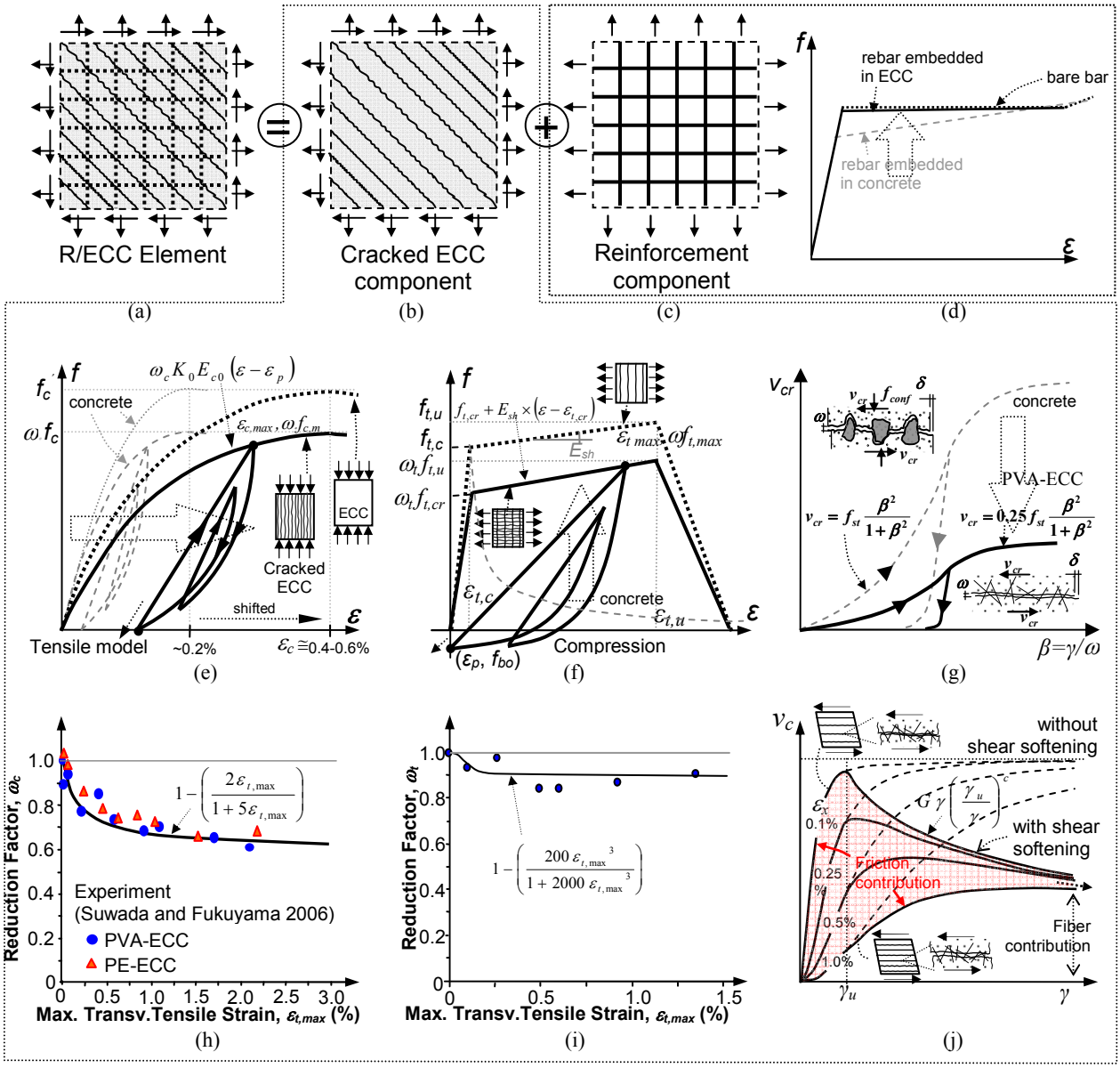

Fig. 2 Material models for R/ECC in the context of a smeared fixed crack approach.

ber anchorage at crack locations in addition to stress non-uniformity that may be caused by a tortuous crack path. The factor is approximated from the strength of pre-cracked ECC plates with dimensions of 250×340×20 mm that were tested using a four point bending scheme (Suryanto 2009). Prior to the tests, the pre-cracks were introduced to the plates by varying the initial tensile strains.

The modeling of shear transfer adopts the shear transfer model for *normal-strength* concrete proposed by Li and Maekawa (1988), which is expressed in terms of shear stress at crack v_{cr} versus crack kinematics β (crack slip-to-crack opening ratio) relationship in the following manner [see **Fig. 2(g)**]

$$v_{cr} = A f_{st} \frac{\beta^2}{1+\beta^2} \tag{1}$$

where v_{cr} is the shear stress transferred across a crack, f_{st} is the maximum shear stress that can be transferred across a crack and is given by $f_{st} = 3.8\, f_c^{'1/3}$ ($f_c^{'}$ in MPa), and β is the ratio of crack slip (γ_{cr}) to crack opening (ε_t). A reduction coefficient A=0.25 is introduced to the model, reflecting that shear transfer resistance in cracked ECC, which contains approximately 2% PVA fibers by volume, is significantly less than that usually provided by aggregate interlock in cracked concrete (A=1.0). The reduction coefficient A was obtained from parametric analyses on the response

of pre-cracked ECC plates subjected to principal stress rotation and R/ECC panel subjected to pure shear in a companion paper (Suryanto *et al* 2010b). A different A value should be used for a different type of fibers and volume fractions. Two components are considered to contribute to shear transfer in cracked ECC: shear friction and fiber bridging. At large shear deformation, it is postulated that the contribution of shear friction progressively diminishes from ultimate shear strain γ_u, while the contribution of the fibers still remains. This is treated as a shear softening phenomenon and is represented with a decay function in which the steepness is controlled with a softening parameter c. To take this into account, the expression proposed by An (1995) is adopted [see **Fig. 2(j)**], as given by

$$v_c = G\gamma\left(\frac{\gamma_u}{\gamma}\right)^c \quad \text{for } \gamma \geq \gamma_u \tag{2}$$

where v_c is the average shear stress, G is the average shear stiffness of cracked PVA-ECC, γ_u is the average shear strain from where the shear softening starts, and c is the shear softening coefficient. It is expected that the values of γ_u and c relates to types and volume of the fibers used in the ECC. For ECC containing approximately 2% PVA fibers by volume and reinforced with uniformly distributed reinforcement, it was found that a value of γ_u=4,000μ gives acceptable agreement. The c parameter is suggested to be 0.4 unless the fiber volume is less than 2% in which a greater c value should be used. **Figure 2(j)**, for clarity, shows the shear transfer response of PVA-ECC for various values of normal strain ε_x.

3. Analysis of R/ECC panels

3.1 R/ECC panels information

Six orthogonally-reinforced R/ECC panels were tested at the University of Toronto by Xoxa (2003) using the available shear rig test facility. The panels were 890 mm square and 70 mm thick and were tested within three to four months after casting. The panel size was comparatively large compared to the PVA fibers length used in the test panels such that it is expected that any size effects would be insignificant. The first three panels (Panel PK1 to PK3) contained the same reinforcement amounts in the two orthogonal directions labeled as isotropic panels, while the other three panels (PK4 to Pk6) contained different reinforcement amounts in the two directions, and were thus labeled as anisotropic panels. Panel PK1 to PK3 were orthogonally reinforced with one layer of reinforcement in each direction. Panels PK4 and PK6 were reinforced with two layers of longitudinal reinforcement and one layer of transversal reinforcement. Panel PK5 were reinforced with two layers of reinforcement in the two orthogonal directions.

Figure 3(a) shows the reinforcement details of Panel PK3. Material properties of the test panels are listed in **Table 1** and **2**, respectively.

Each panel was uniformly stressed over its edge perimeters under a load-controlled condition. All panels, except Panel PK2, were subjected to monotonic pure shear loading until failure. Panel PK2, which has the same design as Panel PK1, was subjected to reverse cyclic pure shear loading. At each loading step, the load was held about constant while the cracks were marked and surface strains were measured. The surface strains were determined from average readings of sixteen Zurich gauge targets as sketched in **Fig. 3(b)**. Additionally, the surface strains were continuously monitored from six LVDTs mounted on each face of the panel. Continuous measurements were also made on the applied loads and the strain profile of several reinforcing bars in the two orthogonal directions. For additional details regarding the experimental program, one should refer to Xoxa (2003).

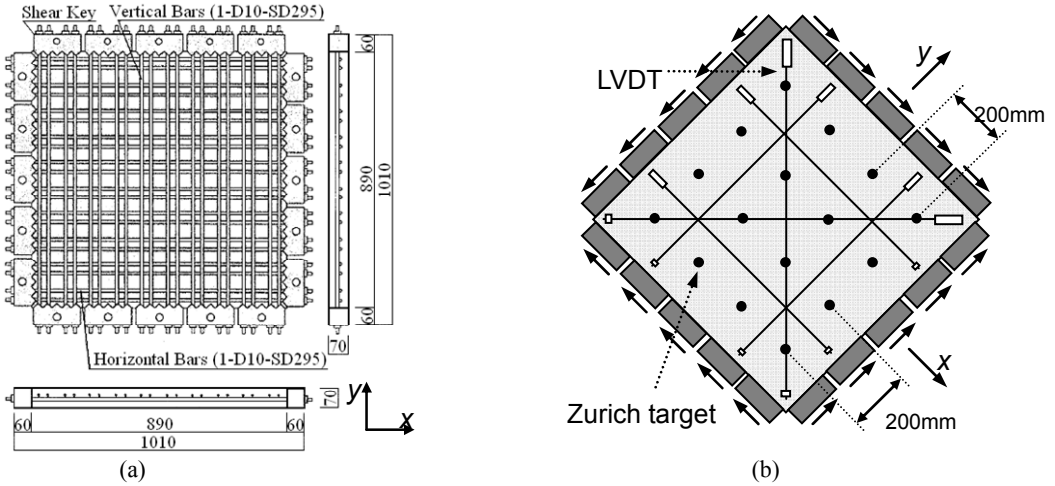

Fig. 3 Details of test panel: (a) Example of reinforcement details of Panel PK3 (Xoxa 2003) and (b) Typical instrumentation of the test panels.

Table 1 Loading condition and material properties of PVA-ECC (Xoxa 2003).

Panel ID	Loading Condition	Elastic Modulus E_c # (GPa)	Comp. Strength f_c' # (MPa)	Ultimate Comp. Strain ε_c' # (%)	X-Direction Reinforcement		Y-Direction Reinforcement	
					Type	ρ_x (%)	Type	ρ_y (%)
PK1	Static	14.8	48.9	0.492	D6	0.514	D6	0.514
PK2	Cyclic	14.8	48.9	0.492	D6	0.514	D6	0.514
PK3	Static	15.8	48.2	0.485	D10	2.280	D10	2.280
PK4	Static	15.5	47.7	0.511	D10	4.560	D6	0.514
PK5	Static	15.4	50.7	0.506	D10	4.560	D6	1.027
PK6	Static	15.8	52.2	0.508	D10	4.560	D6HS	0.514

tested on the same day or one day before the corresponding panel test. The values are the average of three cylinders 100 mm in diameter and 200 mm in height.

Table 2 Material properties of reinforcement (Xoxa 2003).

Rebar Type	Elastic Modulus E_s (GPa)	Yield Strain ε_{sy} (%)	Yield Stress f_y (MPa)	Ultimate Strength f_{su} (MPa)
D6	18.98	0.1941	361.4	493.1
D10	16.62	0.213	334.6	461.8
D6HS	18.86	0.5301	999.6	1149.7

Two distinct types of failure modes were observed from the test panels. Panels PK1, PK2, and PK3 had their ultimate strength after yielding of the longitudinal and transversal reinforcement, most likely because of tensile failure of the ECC. The ultimate strength of Panel PK4 through PK6 were governed by shear sliding failure at the most critical section parallel to the longitudinal reinforcement, which for Panel PK6 was also combined with local edge failure. In all cases, the failure was ductile.

3.2 Finite element modeling and analysis strategy

The models outlined in the earlier part of this paper have been implemented to COM3, a nonlinear finite element program for RC (Maekawa *et* al 2003). In this paper, the program is used to predict the response of the test panels. Since the test panels were uniformly stressed, only a single eight node Mindlin plate element was used to represent both the ECC and the embedded reinforcement. All analyses presented herein employ the two-way fixed crack approach based on the active crack concept. In this approach, nearly orthogonal cracks with the strongest nonlinearity are considered to be the active cracks. Along these cracks, an orthogonal crack coordinate is introduced. At this coordinate, the stress and strain of the ECC are computed. It should be noted that the crack coordinate is introduced after the formation of the first crack.

The analysis presented in this paper can be divided into two parts. The first part presents the results of the test panels, while the second part presents the results for a series of R/ECC panels reinforced with various reinforcement ratios. The objective of the first part is to study factors influencing the behavior of R/ECC, while the second part aims to gain insights on the shear characteristics of R/ECC. Material parameters in all analyses are calibrated against material test data, except for parameters of the tension model, which are determined according to the panel test results.

A custom-based tensile property is used because of considerable variability in tensile responses of the ECC from the panel tests. **Figure 4(a)**, for clarity, shows the tensile stress-strain responses of the ECC extracted from the panel tests, plotted against the average response obtained from direct tensile test. The direct tensile tests were conduced on a dumbbell type specimen with 30×13 mm^2 testing section. Details of a similar tensile test can be found in Kanda *et al* (2006), described as the TC type test. As can be observed from **Fig. 4(a)**, the extracted responses are clearly below the observed response in terms of first cracking, tensile ductility, and tensile strength. The early cracking may be attributed to initial shrinkage-induced stress, while the variations of tensile ductility and strength appear to be sensitive to the arrangement and amount of the reinforcement. Fiber orientation effects may also contribute to the differences since the orientation of fibers in a structural member is usually more random than in a coupon specimen (the coupon specimen is usually much thinner and narrower width). If only direct tensile test data are available, a calibration should be made, particularly when the size of the coupon specimens is much smaller. It appears that the tensile cracking stress, tensile ultimate stress, and tensile ductility should be decreased. A comparison with indirect tensile test methods (e.g.: the JCI method [JCI-S-003-2007], or the one proposed by Qian and Li [2008]) is encouraged.

At this current stage of development, no definite conclusion could be derived from the limited panel test data regarding appropriate tensile property of ECC for R/ECC structural analysis. Here a custom-based tensile property was considered as listed in **Table 3** and shown in **Fig 4(b)**. This custom-based property was determined such that it is comparable to the obtained tensile property from the test panels. The scope of this paper is therefore to verify the proposed models (see Analysis Objective in **Table 3**) and to verify the applicability of

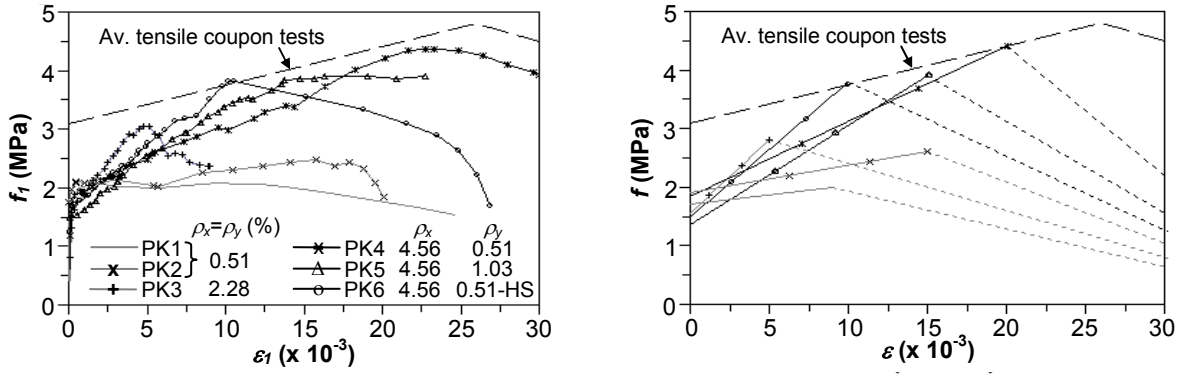

Fig. 4 Principal stress and strain responses of the PK Panels: (a) Tensile stress-strain and (b) Assumed tensile property in analysis.

Table 3 Tensile properties used in the analysis and the corresponding analysis objective.

Panel ID	Crack Stress $f_{t,cr}$ (GPa)	Ultimate Stress $f_{t,u}$ (MPa)	Ultimate Strain $\varepsilon_{t,cr}$ (%)	Strain at Zero Stress $f_{t,o}$ (%)	Analysis Objective
PK1	1.70	2.00	0.9	4.0	Reinforcement model
PK2	1.90	2.60	1.5	4.0	Reinforcement model Hysteretic Tension-Compression model
PK3	1.55	2.80	0.5	4.0	Compression model
PK4	1.85	4.40	2.0	4.0	Shear transfer model
PK5	1.35	3.90	1.5	4.0	Shear transfer model
PK6	1.50	3.80	1.0	4.0	Shear transfer model

other material properties obtained from material tests. If a generalized tensile property could be identified, the models can be further used to predict the hysteretic response of R/ECC structural members (Suryanto *et al.* 2010b).

4. Results and discussions

4.1 Isotropic panels

(1) Panels PK1 and PK2 (ρ_x=ρ_y=0.514%) tested under static and cyclic loading

Since Panels PK1 and PK2 contained relatively low reinforcement ratio, these panels are useful to study appropriate reinforcement model in R/ECC. Two reinforcement models were studied to predict the response of Panel PK1: elastic plastic model–as proposed and a modified reinforcement model incorporating a hardening response during yielding (Salem 1999), which is typically used for RC modeling in accounting for localized steel yielding at cracks. The predictions employing both reinforcement models are shown in **Fig. 5(a)** along with the corresponding experimental data. As can be seen, the prediction with elastic-plastic model is better than that with modified model in terms of the yield point and plate capacity. Since the variations of steel stress at cracks diminish as the reinforcement ratio increases, the results for elastic-plastic model alone are presented for the remaining panels.

To investigate the significance of proper identification of tensile ECC property, the panel was re-analyzed with tensile property according to that obtained from direct tensile tests. As can be seen, the accuracy of the predictions becomes poor. The predicted response deviates significantly from the first cracking, achieves a higher yield load value, and finally reaches peak load and deformation values grossly above the observed values. Thus, it is obvious that a suitable tensile ECC property is critical to correctly predicting the response of R/ECC, particularly in R/ECC member with low amounts of reinforcement as will be discussed in a later part of this paper.

Since Panel PK2 was subjected to cyclic loading and contained a relatively low reinforcement ratio, the analysis of this panel is useful to verify the hysteretic path of the tension-compression models of ECC and to verify, once again, the reinforcement model. The predicted and observed load-deformation response is shown in **Fig. 5(b)**. As can be seen, the predicted response is very consistent with the test observation throughout the loading cycles; both appear to develop a higher degree of stiffness degradation, a larger value of residual displacement, and a more remarkable degree of pinching as the maximum displacement at each load cycle is increased. The close correlation of the two validates the applicability of the hysteretic unloading-reloading formulations of the concrete models that are

adopted in this paper as in the tension and compression models. Slight discrepancy appears only around the yield points in the negative loading direction (peak of Load Cycle 6 and 10) in which the predictions overestimate the load capacity. The potential cause of the discrepancy is explained below.

Observations on the internal stress-strain plotted in **Fig. 5** suggests that Panels PK1 and PK2 failed by tensile failure of the ECC after the yielding of the reinforcement. The compressive stress in the ECC is still well below its compressive strength, even after the largest reduction factor shown previously in **Fig. 2(h)** is applied. It also suggests that the agreement between the computed and observed response of the ECC is good in almost every aspect. For Panel PK2, this includes the history of the compressive stresses and tensile stresses, the re-contact stresses during the cyclic excursion and the flat-top tensile response during the cyclic loading. The flat tensile response is predicted due to the effects of transverse cracking. The only significant difference is the response during the last load cycle in the negative loading direction (load cycle 10). The reloading response, possibly due to extensive damage, shows a curved-shape reloading path, while the predicted response assumes a linear reloading path throughout. For this reason, the predicted load capacity overestimates the observed load capacity. Finally, it is worth noting that the ECC still shows significant tensile stress although it is progressively damaged under cyclic loading reversals.

(2) Panel PK3 (ρ_x=ρ_y=2.28%) tested under static loading

Panel PK3 contained a moderate reinforcement ratio such that the response might be started to be influenced by the accuracy of the ECC modeling in compression. To illustrate the significance of this aspect, two different analysis cases were run. One with compressive strength reduction factor, while the other with no reduction factor. The results are shown in **Fig. 6(a)**. As can be seen, the predicted response accounting for the transverse cracking effects gives a better correlation with the observed response. The effects of transverse cracking on the behavior of the panel are, however, still minor, as marked by a slight reduction in post-cracking shear stiffness. Since the weakening effects of transverse cracking is more pronounced in panels with higher reinforcement ratios, further experiments in such panels appear necessary to validate the proposed reduction factor more comprehensively.

To obtain a better indication on the weakening effects of transverse cracking, the internal compressive stress-strain response is shown in **Fig. 6(b)**. It can be seen that cracked ECC under biaxial tension and compression exhibits lower compressive stress and stiffness than ECC under uniaxial compression. The consideration of the reduction factor in a function of maximum transverse strain enables the modeling of such a behavior reasonably.

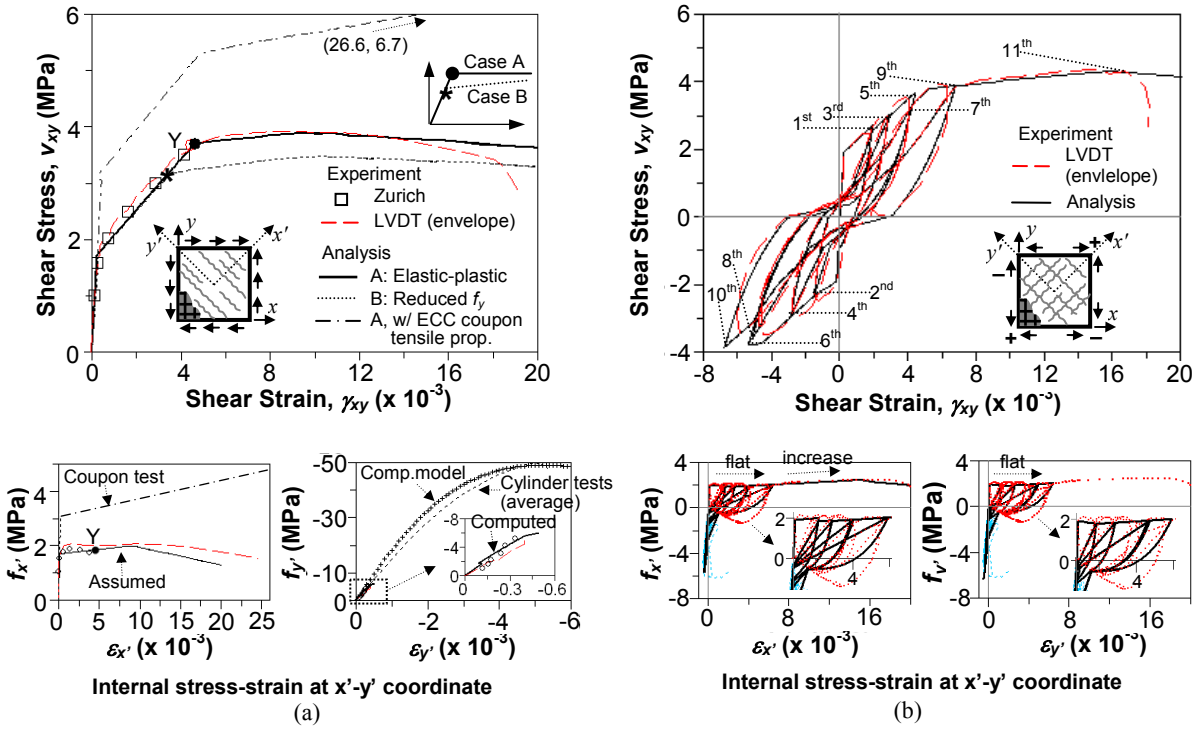

Fig. 5 Comparison of the computed and observed shear stress versus shear deformation of Panels (a) PK1 and (b) PK2 and the corresponding internal stress-strain at x'-y' coordinate.

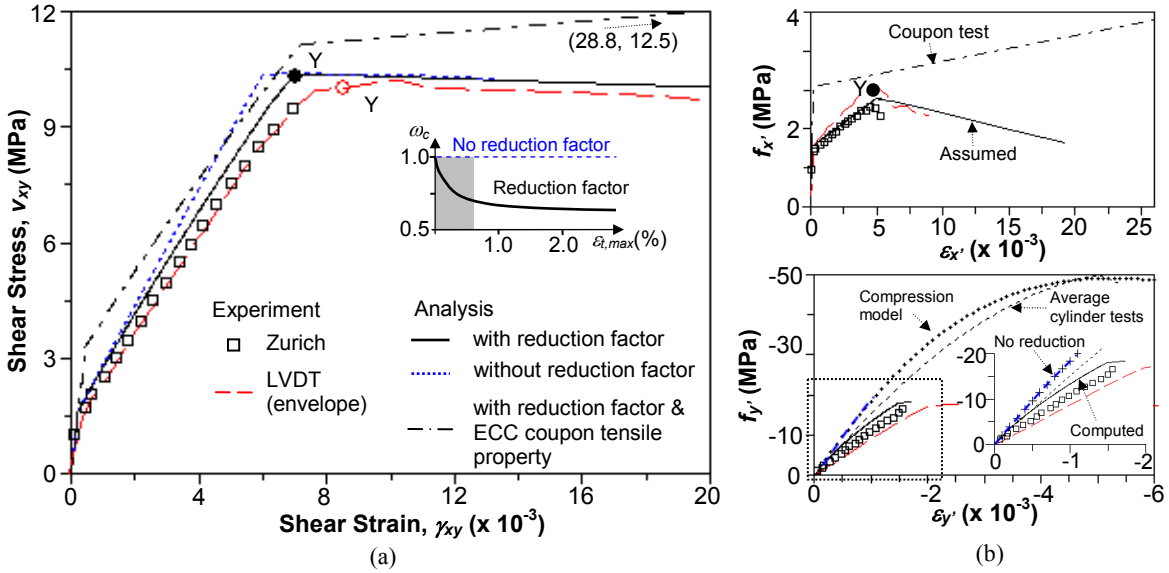

Fig. 6 Load-deformation response of Panel PK3 and the corresponding internal stresses.

4.2 Anisotropic panels: Panels PK4, PK5, and PK6

Panels PK4, PK5, and PK6 exhibited noticeable crack shear slip and significant rotation of principal stress-strain directions owing to the difference in the amount of reinforcements in the two orthogonal directions. In such a condition, correct modeling of shear transfer is critical. To give a quantitative measure on the difference in reinforcement amount, an anisotropy index R is introduced as also used by Xoxa (2003) as given by:

$$R = \frac{\rho_x f_{y,x}}{\rho_y f_{y,y}} \tag{3}$$

where ρ_x and ρ_y are the reinforcement ratio in the x and y directions and $f_{y,x}$ and $f_{y,y}$ are the corresponding yield strength, respectively. The R values for Panel PK4 to PK6 are 8.2, 4.1, and 3.0, respectively, which represents high to moderate anisotropic levels. To clarify the effects of different anisotropic levels on the response of the panels as well as to verify the applicability of the shear transfer model, **Fig. 7** to **Fig. 10** shows the panels responses in terms of load-deformation response, ECC principal compressive stress-strain, average crack shear-strain transfer, and inclination of principal stress versus principal strain direction, respectively.

The predicted and observed load-deformation responses of the panels are shown in **Fig. 7**. It is apparent that as the R value increases the shear capacity decreases, while the shear deformation increases. For all cases, the agreement of the predicted and observed response is reasonably good. Prior to the yielding of the transverse reinforcement, the agreement is good. Soon after yielding, discrepancy between the analysis and experiment becomes more significant as the load is increased and then becomes insignificant as the load attains somewhat near the peak load. The discrepancy around the yielding occurrence is likely attributed to the smeared modeling of the reinforcement, assuming all transverse reinforcements yield instantly when attaining the yield stress. In contrast, it was observed in experiment that not all transverse reinforcements yielded at the same time. In Panel PK5, for example, the first yielding was observed at shear stress of about 6 MPa, while complete yielding had been achieved at shear stress of about 7.5 MPa. This might thus be responsible for the stiff response observed soon after yielding. Failure of the panels is predicted due to shear sliding failure prior to the yielding of the longitudinal reinforcements and after the yielding of the transversal reinforcement, which also agrees to the observed failure mode.

To obtain a better picture on the sliding shear failure, the computed and observed principal compressive stress-strain responses is compared against the corresponding cylinder test results in **Fig. 8**. The agreement of the prediction and observed responses is good; both indicate a significant compressive strength reduction and a significant compressive strain deformation after the yielding of the transverse reinforcement. It is apparent that the compressive strength decreases as the R value increases. The decrease in compression strength is though related with the breakdown of shear transfer mechanisms in the ECC at large shear deformations, and hence results in an extensive shear sliding failure.

To investigate the shear transfer characteristic of the ECC, the average shear stress and average shear strain of the ECC is evaluated. This was done by transforming the stress and strain data of the ECC from the global x-y coordinate to the crack x'-y' coordinate. By doing so, three average stress-strain relationships of ECC can be obtained: tensile stress-strain normal to crack, compressive stress-strain parallel to crack, and shear stress-strain

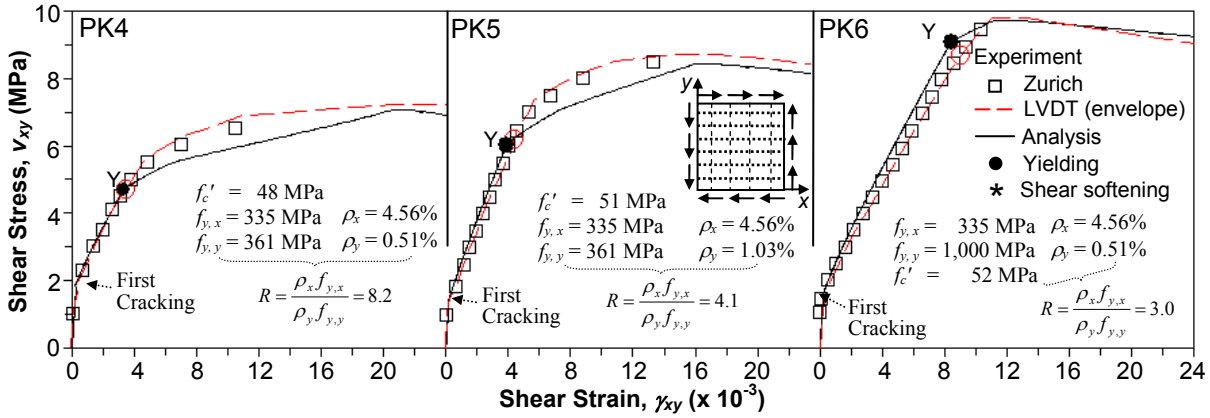

Fig. 7 Load-deformation response of Panels PK4, PK5, and PK6.

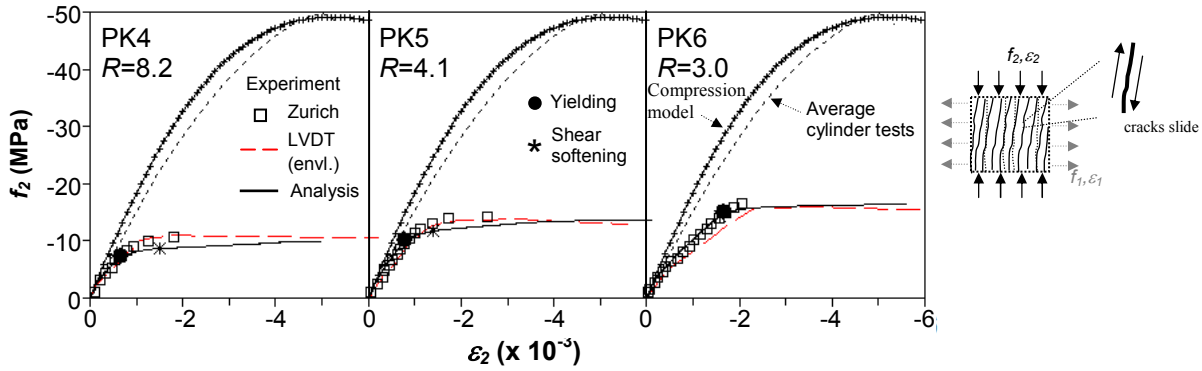

Fig. 8 Comparison of principal compressive stress-strain from the analysis and the experiment to the unixial compressive stress-strain.

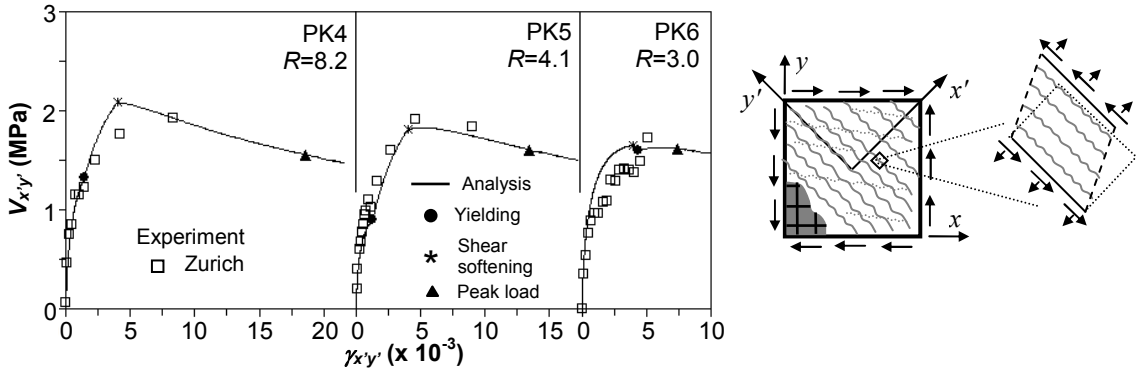

Fig. 9 Comparison of shear stress-strain relation of cracked ECC computed from FEA and extracted from experimental data.

relationships. Presented herein is the average shear stress versus average shear strain relation.

Figure 9 compares the extracted and computed shear stress-strain of the ECC in the crack coordinate. The discrete points correspond to the extracted response, while the line plots correspond to the predicted response. Note that the extracted response was based upon the Zurich data, which are available prior to the ultimate stage only. In all cases, both the predicted and the observed responses are in a similar trend and in a good correlation. This demonstrates the possibility to represent shear transfer behaviors in cracked ECC under various anisotropy conditions with an explicit shear transfer model. The extracted response shown suggests

that the ability of the ECC to transmit shear is limited, as marked by highly nonlinear response at large shear deformations. For this reason, it is crucial to limit the ability of the ECC to transmit shear stress at large shear deformations.

To check how the consideration of shear softening affects the panel response and to study the mechanisms involved during loading, the inclination of principal stress direction and principal strain direction is examined. **Figure 10** compares the inclination angle of the stress and the strain fields versus the applied shear stress obtained from analysis and experiment. From first cracking to yielding of the transverse reinforcement, the predicted inclination angles of the principal stress direction and principal strain direction correlate to the observed angles fairly well. An important aspect to note is that after first cracking the rate of inclination of the strain field is faster than that of the stress field (see Note A in **Fig. 10**). The faster increase of the strain field reflects the occurrence of extensive crack slip. In Panels PK4 and PK5, the shear softening is predicted to occur somewhat after the yielding of the transverse reinforcement, whereas in Panels PK6, it is right before the yielding of transverse reinforcement. The shear softening occurrence is indicated by the shift of the stress field angle back to 45 deg (see the turning point noted by SS in **Fig. 10**). The shift back of the stress field demonstrates that the stress carrying mechanisms involved rely more on the actions of compression and tension and less on crack-shear transfer. This condition continues until the ultimate condition is reached (see Note F in **Fig. 10**). Overall, the predicted stress and strain fields correlates with the observed responses fairly well.

5. Shear strength predictions

To provide further insights on shear characteristics of R/ECC, two series of imaginary R/ECC panels were analyzed. The first series represents a group of isotropic panels with reinforcement ratio varied from zero to six percents. The material property used is those identified from Panels PK1 and PK3. The second series of panels represents a group of anisotropic panels. The longitudinal reinforcement of the panels was set constant at 4.56%, while the transverse reinforcement was varied from zero to six percents. Material properties considered in the analysis were those identified from Panel PK4 through PK6.

Figure 11(a) shows the predicted shear strengths of the isotropic panels. As can be seen from the figure, the normalized shear strength increases almost linearly with increasing amounts of reinforcement ($\rho f_y/f_c'$) up to approximately 0.3, beyond which the gain in strength is not appreciable due to the crushing of the ECC. A significant shear strength can also be observed even with no reinforcement ($\rho f_y/f_c'$ equals to zero). The overall trend is, in general, similar to that of RC panels reported by Vecchio and Collins (1986). Plotted as a dash line also in the figure (Line A) is the predictions neglecting the contribution of the ECC to transmit tensile stresses at cracks. It appears that as the amount of the reinforcement is increased, the contribution of the ECC to the overall shear capacity decreases. In view of this, it seems that the ECC would be more beneficial to be used in R/ECC elements with low reinforcement ratio.

Figure 11(a) also reveals that the predicted shear strengths, which one of them is based on tensile property of either Panel PK1 or PK3, are very close to one another over a wide range of reinforcement ratios. Hence they seem to represent the shear strength of R/ECC in which the ECC contains PVA fibers approximately 2% by volume, as used in the test panels. It should be noted, however, that the predictions are based on limited test data. It would be interesting to have more experimental data to develop a complete understanding of the behavior of R/ECC in shear, particularly when the failure of the panel involves the crushing of the ECC.

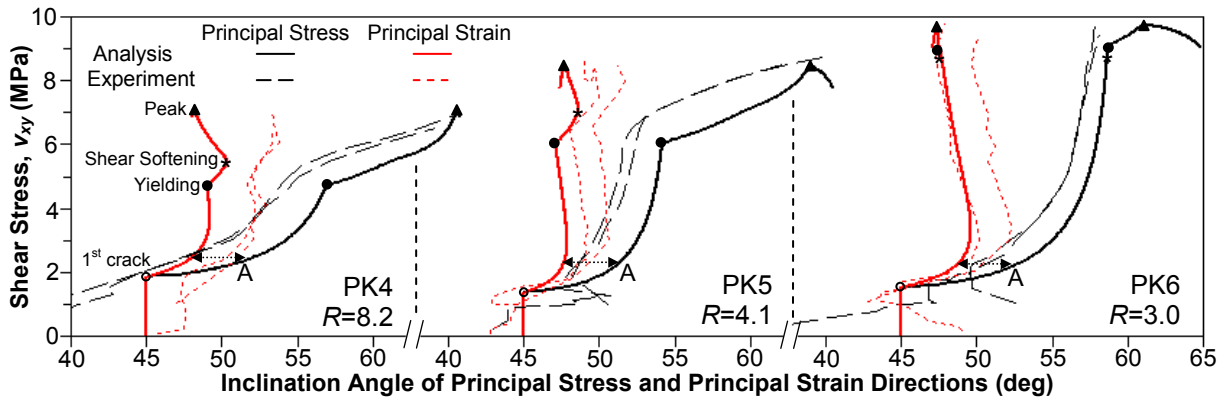

Fig. 10 Comparison of inclination angle of principal stress and principal strain directions obtained from experiment and analysis.

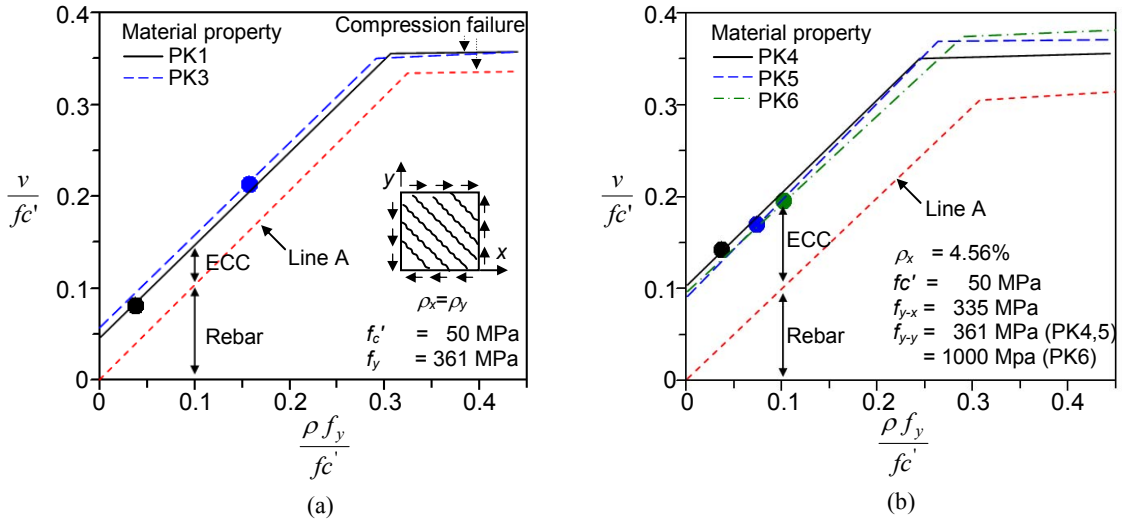

Fig. 11 Shear strength of: (a) isotropicaly reinforced ECC panels and (b) anisotropically reinforced ECC panels.

The predicted shear capacities of the anisotropic panels are shown in **Fig. 11(b)**. Plotted in the figure also is the predictions assuming that the ECC does not have the ability to transmit tensile stresses and shear stresses at cracks. As $\rho_y f_y/f_c'$ increases, shear capacity also increases with the maximum value for $\rho_y f_y/f_c'$ equals to approximately 0.275, while the contribution of the ECC to the overall shear capacity decreases. By comparing the predicted shear capacities for each $\rho_y f_y/f_c'$ value to those shown in **Fig. 11(a)**, it is apparent that the contribution of the ECC to the overall shear capacity increases when the amount of the reinforcement in the two orthogonal directions is different. The tendency shown suggests that adding longitudinal reinforcement is effective to increase shear capacity in R/ECC. Further experiments in reversed cyclic shear loading are encouraged to validate this beneficial effect as reversed loading can cause rubbing of crack surfaces in the ECC that may subsequently damage the fiber bridging across cracks.

6. Conclusions

Verification of this analytical framework for analysis of R/ECC is presented. The framework is in the context of a smeared, fixed crack approach that employs three smeared models for ECC: compression, tension, and shear transfer models, and one model for reinforcement. The applicability of the models is verified using experiments on six R/ECC panels subjected to pure shear, demonstrating that the proposed models replicate essential responses of the plates well. The experimental data highlight an important aspect that should be considered: the actual tensile property of the ECC in a R/ECC member may differ remarkably from that obtained from direct tensile tests due to several influencing factors, and hence it should *not* be directly used for a simulation. Obviously, an objective measure of the tensile property of ECC in different R/ECC members is desirable and should be an important topic for future research. Using the identified tensile property from the panel tests, a series of analysis was performed in this paper to validate the accuracy of the analytical framework presented. The following conclusion can be derived from this analysis:

(1) It appears necessary to account for reductions in strength due to transverse cracks for modeling hysteretic compression and tension responses of ECC. On the other hand, it appears unnecessary to account for reductions in yield stress for representing reinforcement when embedded in ECC.

(2) ECC nonlinearity plays a significant part in the response of a lightly reinforced ECC panel subjected to reversed cyclic loading that leads to significant changes in load-deformation stiffness, residual strains, and degree of pinching as the maximum deformation at each load cycle is increased. All of these aspects are represented by the proposed models adequately.

(3) Employing a decay function to limit the ability of ECC to transmit shear stresses is shown to be effective in accounting for the breakdown of shear transfer mechanism in ECC at large shear deformations. With this decay function, the snap back angle of the stress field observed from the anisotropic test panels can be rationally explained. The resulting shear transfer model is shown replicating the average shear transfer response of three anisotropic panels with different anisotropy levels well. This confirms that an explicit representation of shear transfer of cracked ECC is achievable.

(4) The analysis results show that the main cause of the lag angle between the principal stress and principal strain directions and the sliding shear

failure observed in the anisotropic panels is the ease of the pre-existing cracks to slip.

(5) The contribution of ECC to the overall R/ECC shear capacity is greater in low reinforcement ratios, where it would be more beneficial to be used. Shear capacity is found to increase with the increase amount of longitudinal and transversal reinforcements. However, concerns have to be made to use the ECC in a high reinforcement ratios (e.g.: $\rho f_y/f_c' > 0.275$) due to the crushing of the ECC.

Acknowledgments

The first author wishes to express his gratitude to the Ministry of Education, Culture, Sports, Science and Technology and the Japan Society for Promotion of Science (JSPS) for the scholarship and fellowship that enabled him to carry out this study. The authors would also express their gratitude to Dr. Tetsushi Kanda for his valuable comments and discussions.

References

An, X. (1995). "Failure analysis and evaluation of seismic performance for reinforced concrete in shear." Thesis (PhD). University of Tokyo.

Cervenka, V. (1985). "Constitutive model for cracked reinforced concrete." *Journal of the ACI*, 82(6), 877-882.

Fischer, G. and Li, V. C. (2002). "Influence of matrix ductility on tension-stiffening behavior of steel reinforced Engineered Cementitious Composites (ECC)." *ACI Structural Journal*, 99(1), 104-111.

Han, T. S., Feenstra, P. H. and Billington, S. L. (2003). "Simulation of highly ductile fiber-reinforced cement-based composite components under cyclic loading." *ACI Structural Journal*, 100(6), 749-757.

Hung, C. C. and El-Tawil, S. (2009). "Cyclic model for High Performance Fiber Reinforced Cementitious Composite structures." *In*: B. Goodno, Ed. *The 2009 ATC&SEI Conference on Improving the Seismic Performance of Existing Buildings and Other Structures*, San Francisco *9-11 December 2009*. ASCE, 1341-1352.

JCI-S-003-2007. (2007). "Method of test for bending moment-curvature curve of fiber-reinforced cementitious composites." *Japan Concrete Institute Standard*, 7.

Kanda, T., Tomoe, S., Nagai, S., Maruta, M., Kanakubo, T. and Shimizu, K. (2006). "Full scale processing investigation for ECC pre-cast structural element." *Journal of Asian Architecture and Building Engineering*, 5(2), 333-340.

Kato, B. (1979). "Mechanical properties of steel under load cycles idealizing seismic action." *CEB Bulletin D' Information*, 131, 7-27.

Kaufmann, W. and Marti, P. (1998). "Structural concrete: cracked membrane model." *Journal of Structural Engineering*, 124(12), 1467-1475.

Li, B., Maekawa, K. and Okamura, H. (1989). "Contact density model for stress transfer across cracks in concrete." *Journal of the faculty of engineering*, the University of Tokyo (B), 40(1), 9-52.

Maekawa, K., Pimanmas, A. and Okamura, H. (2003). "*Nonlinear mechanics of reinforced concrete*." London: Spon Press.

Qian, S. and Li, V. C. (2008). "Simplified inverse method for determining the tensile properties of strain hardening cementitious composites (SHCC)." *Journal of Advanced Concrete Technology*, 6(2), 353-363.

Salem, H. and Maekawa, K. (1999). "Spatially averaged tensile mechanics for cracked concrete and reinforcement in highly inelastic range." Concrete Library of JSCE, 34, 151-169.

Suryanto, B. (2009). "Mechanics of high performance fiber reinforced cementitious composite (HPFRCC) under principal stress rotation." Thesis (PhD), University of Tokyo.

Suryanto, B., Nagai, K. and Maekawa, K. (2010a). "Bidirectional multiple cracking tests on HPFRCC plates." *ACI Material Journal*, 107(5), 450-460.

Suryanto, B., Nagai, K. and Maekawa, K. (2010b). "Modeling and analysis of shear-critical ECC members with anisotropic stress and strain fields." *Journal of Advanced Concrete Technology*, 8(2), 239-258.

Suwada, H. and Fukuyama, H. (2006). "Nonlinear finite element analysis on shear failure of structural elements using High Performance Fiber Reinforced Cement Composite." *Journal of Advanced Concrete Technology*, 4(1), 45-57.

Vecchio, F. J. and Collins, M. P. (1982). "The response of reinforced concrete to in-plane shear and normal stresses." Rep. No. 82-03, Dept. of Civil Engineering, Univ. of Toronto, Toronto.

Vecchio, F. and Collins, M. P. (1986). "The modified compression field theory for reinforced concrete elements subjected to shear." *Journal of the ACI*, 83(2), 219-231.

Vecchio, F. J., Collins, M. P. and Aspiotis, J. (1994). "Response of high strength concrete elements in shear." *ACI Structural Journal*, 91(4), 423-433.

Xoxa, V. (2003). "Investigating the shear characteristics of high performance fiber reinforced concrete." Thesis (Master). University of Toronto.